

ADAPTIVE GRAPH CONVOLUTIONAL NETWORKS FOR WEAKLY SUPERVISED ANOMALY DETECTION IN VIDEOS

Congqi Cao, Xin Zhang, Shizhou Zhang, Peng Wang, Yanning Zhang

ASGO National Engineering Laboratory, Northwestern Polytechnical University

Email: {congqi.cao, szzhang, peng.wang, ynzhang}@nwpu.edu.cn; zhangxin_@mail.nwpu.edu.cn

ABSTRACT

For the weakly supervised anomaly detection task, most existing work is limited to the problem of inadequate video representation due to the inability to model long-time contextual information. We propose a weakly supervised adaptive graph convolutional network (WAGCN) to model the contextual relationships among video segments. And we fully consider the influence of other video segments on the current segment when generating the anomaly probability score for each segment. Firstly, we combine the temporal consistency as well as feature similarity of video segments for composition, which makes full use of the association information among spatial-temporal features of anomalous events in videos. Secondly, we propose a graph learning layer in order to break the limitation of setting topology manually, which adaptively extracts sparse graph adjacency matrix based on data. Extensive experiments on two public datasets (*i.e.*, UCF-Crime dataset and ShanghaiTech dataset) demonstrate the effectiveness of our approach.

Index Terms—Anomaly detection, temporal modeling, graph neural networks

1. INTRODUCTION AND RELATED WORKS

With the increasing awareness of security and the growing popularity of surveillance cameras in public places, there is an urgent need to develop a technology that can automatically detect and raise alarms for abnormal events in surveillance video. Events in the real world are complex and diverse, and fine-grained annotation of training datasets takes a lot of time and effort. So weakly supervised anomaly detection (WSAD) becomes a popular research area. WSAD has been formulated as a Multiple Instance Learning (MIL) task [1] in prior works. Sultani *et al.* [1] constructed a large-scale anomaly dataset and proposed to use deep MIL ranking loss to separate the anomaly scores of anomalous and normal instances. Subsequently, several improved approaches were developed [2][3][4]. Zhou *et al.* [7] proposed that each example in MIL is not independently and identically distributed, and there is a certain connection among them. However, the above methods ignore the spatial-temporal connection among video segments.

In recent years, several works have applied graph convolutional networks (GCN-s) [8][9][10][11] over the graph to model relations among different nodes and learn powerful video representations. Zhong *et al.* [5] used GCN to denoise normal segments in anomalous videos, and trained 3D convolutional neural networks [12] with the obtained pseudo-labels for anomaly detection. However, in the test phase the model only used current information despite capturing long-range temporal dependencies of the full video in the training phase. And the denoising process may clean up the anomalies, resulting in information loss. Wu *et al.* [6] proposed a GCN with three parallel branches capturing long-range dependencies, local positional relation and the proximity of the predicted scores to describe different relationships among video segments respectively. However, three independent branches cannot model complex relationships coupled together in the video effectively and lead to slow iterative optimization. In addition, there are no learnable parameters in the adjacency matrix of the graph, so the defined graphs may not be suitable for anomaly detection tasks.

In summary, the following challenges have been observed in using GCN to model temporal contextual information, (1) Only one network structure is used to model one type of relationship, or multiple independent branches are used to model different types of relationships separately, which cannot model multiple relationships coupled together within a sequence effectively. (2) Existing GCN methods ignore the fact that self-defined graph structures are not optimal and should be updated during the training process. In this paper, we propose an adaptive GCN to overcome these challenges, and our framework is shown in Figure 1. For challenge 1, we use temporal consistency graph to describe the intrinsic association relationships of features in the smooth undulating interval of an event occurrence. And we use feature similarity graph to express the intrinsic association relationships of video segment features with explicit anomalous events. However, both single temporal consistency GCN and single feature similarity GCN are not optimal to anomalous event detection and localization. In order to make better use of the intrinsic correlations among segments, we integrate the two perspectives to jointly construct a global graph for spatial-temporal feature learning of events.

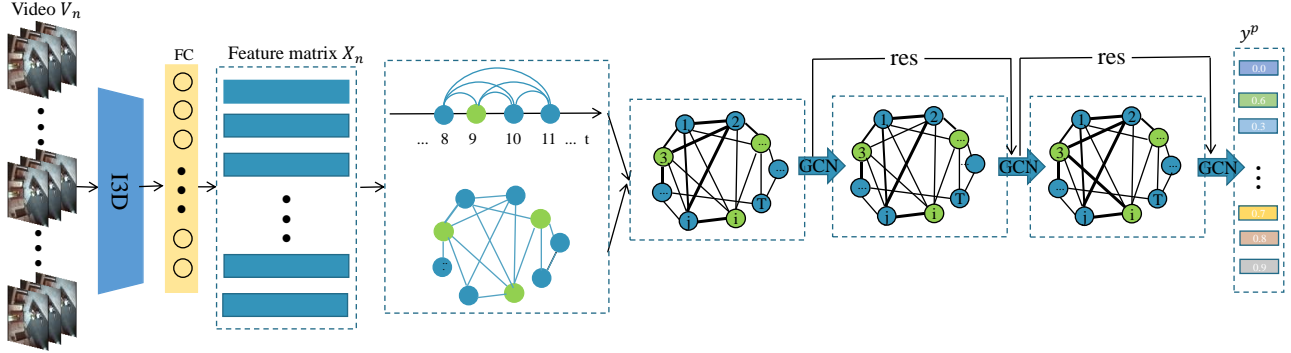


Figure 1 Our proposed WAGCN receives a $T \times D$ feature matrix X_n extracted from video V_n . Then, we construct a global graph to capture the long and short-range temporal dependencies among segments features. Next, we train adaptive GCN using the *top-k* largest anomaly probability scores from abnormal and normal videos.

For challenge 2, during the construction of the adjacency matrix, we break the limitation of manual setting. We consider the similarity among spatial-temporal features of video segments and other potential contextual semantic relationships to learn a video content-adaptive graph adjacency matrix. Moreover, GCN suffer from over-smoothing problem, where the representations of all nodes converge to a smooth point, making them independent of the input features and causing the gradient to vanish. We adopt to add residual connection [13] in GCN to solve this problem. In summary, our main contributions are as follows:

- the construction of a global graph from the similarity of video segments' spatial-temporal features and the degree of video segments' temporal proximity to better exploit the intrinsic correlations among segments;
- the adjacency matrix of the graph is learned adaptively in an end-to-end manner to increase the flexibility of the model-building graph;
- the introduction of residual connection to solve over-smoothing problem.

2. PROPOSED METHOD

2.1. Feature Extraction

The training set has N training videos $\{V_n\}_{n=1}^N$ and corresponding weakly supervised labels $\{y_n\}_{n=1}^N$, where $y_n \in \{0,1\}$. $y_n = 1$ indicates that V_n contains at least one anomalous segment, but no temporal location annotation is provided. $y_n = 0$ means that V_n is entirely comprised of normal segments. Following the earlier MIL-based anomaly detection method [1], the video V_n is divided into a fixed number of non-overlapping segments before each V_n is fed to the feature extractor, and we denote the number of segments by T_n . The Inflated 3D (I3D) [14] pretrained on the Kinetics dataset is used as the feature extraction network to extract the appearance and motion information of the video. The feature matrix X_n is composed of features from video V_n . The dimension of X_n is $T_n \times D$, where D denotes the dimension of segment features.

2.2. Graph Construction Module

Anomalous events occur in a continuous period of time and have a consistent behavior pattern over a period of time. Thus, in order to better model the temporal relationship of the video and better express the dynamic characteristics of the video, we combine the similarity of video segments' spatial-temporal features and the degree of video segments' temporal proximity to construct graph.

2.2.1 Feature similarity graph

Features from the feature extractor first go through a fully connected layer to decrease the feature dimension, in order to mitigate the curse of dimensionality. We propose to construct a feature similarity graph F with graph learning layer to extract the similarity among segments adaptively. We consider capturing dynamic spatial-temporal dependencies. In other words, instead of customizing the weights of the two connected nodes based on the node inputs directly, we dynamically adjust them as the model is trained. Once the model is trained in the online learning version, our graph adjacency matrix can also be adapted to change as the model's parameters are updated with new training data.

We represent the pairwise relations between every two segments in the graph as follows. Since an adjacency matrix should be non-negative, we bound the similarity to the range $(0, 1]$ with a normalized exponential function. Therefore, the adjacency matrix A^F is defined as:

$$A^F = \text{SoftMax}(\tanh(XW_1)\tanh(W_2^T X^T)) \quad (1)$$

where the parameter W_1 and W_2 are $d \times d$ dimension weights which are learnable via back propagation. So, the elements of A^F are parameterized and optimized along with the other parameters during the training process.

2.2.2 Temporal consistency graph

For most anomalous videos, not all anomalous segments are similar to explosive events which happen so drastically.

Instead, they require an undulating process time. As pointed out in [15][16][17], temporal consistency contributes to many video-based tasks. The temporal consistency graph T is built directly on the temporal structure of the video. Its adjacency matrix $A^T \in R^{N \times N}$ depends only on the temporal position of the i -th and j -th segments:

$$A_{ij}^T = \exp(-|i - j|) \quad (2)$$

For the j -th segment, the closer to the i -th segment, the greater the weight assigned to it, which can better reflect the influence of that segment on the i -th segment.

2.3. Graph Convolutional Module

To explore and exploit relationships among segments, we use GCN to model the relationships among segments. Specifically for the k -th layer, the graph convolution is implemented by

$$X^k = \sigma(W^k X^{k-1} (A^F + A^T) + X^{k-1}) \quad (3)$$

where $X^{k-1} \in R^{N \times d_m}$ are the hidden features for all segments at layer $k-1$, and d_m is the dimension of features. $W^k \in R^{d_m \times d_m}$ is a trainable parametric matrix, and σ represents the activation function.

In addition, a residual connection similar to [13] is added to each layer to solve the over-smoothing of the graph, which allows inserting the layer into any existing model without destroying its initial behavior. If the number of input channels is different from the number of output channels, a 1×1 convolution is inserted in the residual path to transform the input to match the output in the channel dimension.

2.4. Training Loss of the Proposed Algorithm

As mentioned before, each video only has normal or abnormal video-level labels. Obviously segments with large abnormal scores in the abnormal video is more likely to be abnormal segments, while segments with large abnormal score in the normal segment is still normal segments. In order to expand the inter-class distance between abnormal and normal segments under weak supervision, we use k -max loss function [4].

Specifically, given the abnormal score $s = \{s_i\}_{i=1}^T$ of video V , we choose the $top-k$ elements in s denoted as $S = \{s_i\}_{i=1}^k$, where $k = \left\lfloor \frac{T}{8} + 1 \right\rfloor$.

The final classification loss is the binary cross-entropy between the predicted label and the ground truth on the training video, which is given by:

$$L_{k\text{-max}} = \frac{1}{k} \sum_{s_i \in S} [-y \log(s_i) + (1 - y) \log(1 - s_i)] \quad (4)$$

3. EXPERIMENTAL RESULTS

3.1. Datasets

UCF-Crime is a large-scale dataset consisting of long untrimmed surveillance videos [1]. It covers 13 real-world

anomalies, including Abuse, Arrest, Arson, Assault, Accident, Burglary, Explosion, Fighting, Robbery, Shooting, Stealing, Shoplifting, and Vandalism. All videos are divided into two parts: the training set consisting of 800 normal and 810 anomalous videos, and the testing set including the remaining 150 normal and 140 anomalous videos.

ShanghaiTech is a medium-sized dataset containing 437 videos, with an average of 726 frames per video. The dataset includes 130 abnormal events in 13 scenes collected at ShanghaiTech University, with complex lighting conditions and camera angles. In order to make it suitable for evaluating weakly supervised binary classification methods, Zhong *et al.* [5] split the data into two subsets: the training set which is made up of 175 normal and 63 anomalous videos, and the test split which contains 155 normal and 44 anomalous videos.

3.2. Evaluation Metrics

Following previous work, we use the frame-level receiver operating characteristic curve (ROC) and corresponding area under the curve (AUC@ROC) to evaluate the performance of our proposed method and comparison methods.

3.3. Implementation Details

Following [1], each video is divided into 32 video snippets, *i.e.*, $T = 32$. The FC layers described in the model have 512 nodes, and the GCN layers described in the model have 128, 32 and 1 nodes, where each of those layers except the last layer is followed by a ReLU activation function and a dropout function with a dropout rate of 0.6. The last layer is followed by a Sigmoid activation function. The 2048-D features are extracted from the “mix 5c” layer of the pre-trained I3D [14]. Our method is trained in an end-to-end manner using the Adam optimizer with a weight decay of 0.0005 and a batch size of 64 for 100 epochs. The learning rate is set to 0.001. Each mini-batch consists of 32 samples from randomly selected normal and abnormal videos.

3.4. Experimental Results and Discussions

We compare our method with the currently available methods on two datasets. The results on the UCF-Crime dataset are shown in Table 1. Noticeably, using the same I3D-RGB features, our method outperforms the previous graph convolution network-based methods, Zhong *et al.* [5] by 1.42%, Wu *et al.* [6] by 0.7%. Furthermore, our method outperforms the supervised method proposed by Liu *et al.* [18], which adds temporal and spatial labels to the UCF-Crime dataset and trains Convolutional 3D Network (C3D) [12] and Non-local Network (NLN) [19] for anomaly detection. These results validate that our proposed method is more effective than previous work. The method RTFM proposed in [21] is superior to our method because it uses feature magnitude to recognize anomalies instead of using classification scores, which enables a stronger learning ability.

Table 1: AUC performance comparison on UCF-Crime. The results with \dagger are re-implemented with I3D features.

Method	Feature	AUC (%)
Sultani <i>et al.</i> [1]	C3D RGB	75.41
Sultani <i>et al.</i> [1] \dagger	I3D RGB	76.92
Zhang <i>et al.</i> [2]	C3D RGB	78.66
Motion-Aware [3]	PWC Flow	79.00
Liu <i>et al.</i> [18]	C3D RGB	70.1
Liu <i>et al.</i> [18]	NLN RGB	82.0
Zhong <i>et al.</i> [5]	C3D RGB	81.08
AR_Net [4] \dagger	I3D RGB	78.96
Wu <i>et al.</i> [6]	I3D RGB	82.44
CLAWS [20]	C3D RGB	83.03
MIST [22]	I3D RGB	82.30
RTFM [21]	I3D RGB	84.03
Ours	I3D RGB	83.14

Table 2: AUC performance comparison on ShanghaiTech. The result with \dagger is re-implemented with I3D features.

Method	Feature	AUC (%)
Sultani <i>et al.</i> [1] \dagger	I3D RGB	85.32
Zhang <i>et al.</i> [2]	C3D RGB	82.50
Zhong <i>et al.</i> [5]	C3D RGB	76.44
AR_Net [4]	I3D RGB & I3D Flow	91.24
CLAWS [20]	C3D RGB	89.67
MIST [22]	I3D RGB	94.83
RTFM [21]	I3D RGB	97.21
Ours	I3D RGB	95.02
Ours	I3D RGB & I3D Flow	95.87

In addition, feature magnitude learning together with anomaly classification can optimize the feature representation space and anomaly classification output space to have large margins between abnormal and normal segments. We will also enhance the discriminative power of the learned features by adding feature magnitude learning to improve the performance of our model in the future.

The frame-level AUC results on ShanghaiTech dataset are shown in Table 2. Our method achieves better performance compared to previous weakly supervised learning methods [1]. Our method is 10.58% better than the GCN-based weakly supervised method [5], which indicates that our GCN module can capture the temporal dependence more effectively. Using the same features (*i.e.*, combining I3D RGB and I3D Flow), our method outperforms the previous MIL-based method with the best performance [4] by 4.6%.

3.5. Ablation Study

To verify the efficiency of our proposed graph adjacency matrix A^F construction method, we use different methods for ablation experiments. Dynamic-A1 that we used is shown in Equation 1. Motivated by [24], Dynamic-A2 is shown in Equation 5. Global-A assumes that the adjacency matrix is a parameter matrix, which contains N^2 parameters. Csim-A is

Table 3: AUC comparison of different graph adjacency matrix A^F construction methods on UCF-Crime.

Dyna mic- A1	Dyna mic- A2	Global -A	Csim- A	Jsim -A	AUC (%)
\checkmark					0.8314
	\checkmark				0.8293
		\checkmark			0.8222
			\checkmark		0.8284
				\checkmark	0.8255

Table 4: AUC comparison of different graphs on UCF-Crime.

Method	AUC (%)
feature similarity graph	0.8196
temporal consistency graph	0.8203
average graph result	0.8234
global graph	0.8314

computed by the cosine similarity scores of segment features. Motivated by [23], Jsim-A is computed by the Jaccard similarity scores of segment features. According to Table 3, dynamic construction of A^F achieves the best performance. Constructing the adjacency matrix dynamically in different ways has little effect on the model performance, but both are better than the adjacency matrix that is constructed fixed at the beginning. If the graph structure does not depend on the input features of nodes at all, the final result is inferior, probably because the fixed design about the graph learning layer is limitative in learning.

$$A_{(i,j)} = \frac{e^2(x_i, x_j)}{\sum_{j=1}^N e^2(x_i, x_j)}, e(x_i, x_j) = (wx_i)^T wx_j \quad (5)$$

To verify the efficiency of constructing a global graph, we construct feature similarity graph and temporal consistency graph to train two independent branches and average the results for comparison. The performance results on UCF-Crime dataset are shown in Table 4. It can be observed that constructing a global graph is more capable of expressing the complex relationships coupled together among video segments.

4. CONCLUSIONS

In this work, we propose an adaptive graph convolutional network for video anomaly detection. The proposed method constructs a global graph considering both feature similarity and temporal disparity. Moreover, a graph learning layer is introduced to construct connections among segments in a video adaptively, which can capture spatial-temporal relationships among video segments effectively and enhance current temporal features. Extensive experiments on two typical datasets show that the proposed method achieves a high level of performance for video anomaly detection.

5. REFERENCES

- [1] Waqas Sultani, Chen Chen, and Mubarak Shah, “Real-World Anomaly Detection in Surveillance Videos,” in *Proceedings of the IEEE conference on computer vision and pattern recognition*, 2018, pp. 6479–6488.
- [2] J. Zhang, L. Qing, and J. Miao, “Temporal convolutional network with complementary inner bag loss for weakly supervised anomaly detection,” in *IEEE International Conference on Image Processing (ICIP)*, 2019, pp. 4030-4034.
- [3] Yi Zhu and Shawn Newsam, “Motion-aware feature for improved video anomaly detection,” in *British Machine Vision Conference (BMVC)*, 2019.
- [4] B. Wan, Y. Fang, X. Xia, and J. Mei, “Weakly supervised video anomaly detection via center guided discriminative learning,” in *IEEE International Conference on Multimedia and Expo (ICME)*, 2020, pp. 1–6.
- [5] J.-X. Zhong, N. Li, W. Kong, S. Liu, T. H. Li, and G. Li, “Graph convolutional label noise cleaner: Train a plug-and-play action classifier for anomaly detection,” in *Proceedings of the IEEE conference on computer vision and pattern recognition*, 2019, pp. 12237–1246.
- [6] Peng Wu, Jing Liu, Yujia Shi, Yujia Sun, Fangtao Shao, Zhaoyang Wu, and Zhiwei Yang, “Not only look, but also listen: Learning multimodal violence detection under weak supervision,” in *European Conference on Computer Vision*, 2020, pp. 322-339.
- [7] Zhihua Zhou, Yuyin Sun and Yufeng Li, “Multi-instance learning by treating instances as non-iid samples,” in *Proceedings of the 26th annual international conference on machine learning*, 2009.
- [8] Xiaolong Wang and Abhinav Gupta, “Videos as space-time region graphs,” in *European Conference on Computer Vision*, 2018, pp. 399-417.
- [9] Y. Song, Z. Zhang and L. Wang, “Richly Activated Graph Convolutional Network for Action Recognition with Incomplete Skeletons,” in *IEEE International Conference on Image Processing (ICIP)*, 2019, pp. 1-5.
- [10] L. Shi, Y. Zhang, J. Cheng, H. Lu, “Two-stream adaptive graph convolutional networks for skeleton-based action recognition,” in *Proceedings of the IEEE conference on computer vision and pattern recognition*, 2019, pp. 12026-12035.
- [11] C. L. Yang, A. Setyoko, H. Tampubolon, *et al.*, “Pairwise adjacency matrix on spatial temporal graph convolution network for skeleton-based two-person interaction recognition,” in *IEEE International Conference on Image Processing (ICIP)*, 2020, pp. 2166-2170.
- [12] Du Tran, Lubomir Bourdev, Rob Fergus, Lorenzo Torresani, and Manohar Paluri, “Learning spatiotemporal features with 3d convolutional networks,” in *Proceedings of the IEEE/CVF International Conference on Computer Vision*, 2015, pp. 4489-4497.
- [13] Kaiming He, Xiangyu Zhang, Shaoqing Ren, and Jian Sun, “Deep Residual Learning for Image Recognition,” in *Proceedings of the IEEE conference on computer vision and pattern recognition*, 2016, pp. 770-778.
- [14] Joao Carreira and Andrew Zisserman, “Quo vadis, action recognition? a new model and the kinetics dataset,” in *Proceedings of the IEEE conference on computer vision and pattern recognition*, 2017, pp. 6299–6308.
- [15] Dinesh Jayaraman and Kristen Grauman, “Slow and steady feature analysis: higher order temporal coherence in video,” in *Proceedings of the IEEE conference on computer vision and pattern recognition*, 2016, pp. 3852-3861.
- [16] L. Wang, Y. Xiong, Z. Wang, Y. Qiao, D. Lin, X. Tang, and L. Van Gool, “Temporal segment networks: Towards good practices for deep action recognition,” in *European Conference on Computer Vision*, 2016, pp. 20-36.
- [17] Sujoy Paul, Sourya Roy, and Amit K Roy-Chowdhury, “WTALC: Weakly-supervised temporal activity localization and classification,” in *European Conference on Computer Vision*, 2018, pp. 563-579.
- [18] Kun Liu and Huadong Ma, “Exploring background-bias for anomaly detection in surveillance videos,” in *Proceedings of the 27th ACM International Conference on Multimedia*, 2019.
- [19] X. Wang, R. Girshick, A. Gupta, K. He, “Non-local neural networks,” in *Proceedings of the IEEE conference on computer vision and pattern recognition*, 2018, pp. 7794-7803.
- [20] M. Z. Zaheer, A. Mahmood, M. Astrid, *et al.*, “CLAWS: Clustering assisted weakly supervised learning with normalcy suppression for anomalous event detection,” in *European Conference on Computer Vision*, 2020, pp. 358-376.
- [21] Yu Tian, Guan-song Pang, Yuan-hong Chen, *et al.*, “Weakly-supervised Video Anomaly Detection with Robust Temporal Feature Magnitude Learning,” in *Proceedings of the IEEE/CVF International Conference on Computer Vision*, 2021, pp. 4975-4986.
- [22] Jia-Chang Feng, Fa-Ting Hong, and Wei-Shi Zheng, “Mist: Multiple instance self-training framework for video anomaly detection,” in *Proceedings of the IEEE conference on computer vision and pattern recognition*, 2021, pp. 14009-14018.
- [23] Fernando, Basura, and Samitha Herath, “Anticipating human actions by correlating past with the future with Jaccard similarity measures,” in *Proceedings of the IEEE conference on computer vision and pattern recognition*, 2021, pp. 13224-13233.
- [24] Yang, Jinrui, *et al.*, “Spatial-temporal graph convolutional network for video-based person re-identification,” in *Proceedings of the IEEE conference on computer vision and pattern recognition*, 2020, pp. 3289-3299.